Protein composition of the occlusion bodies of *Epinotia aporema* granulovirus

Tomás Masson, María Laura Fabre, María Leticia Ferrelli, Matías Luis Pidre, Víctor Romanowski.

1 Instituto de Biotecnología y Biología Molecular (IBBM, UNLP-CONICET), Facultad de Ciencias Exactas, Universidad Nacional de La Plata, La Plata, Buenos Aires, Argentina.

Abstract

Within family *Baculoviridae*, members of the *Betabaculovirus* genus are employed as biocontrol agents against lepidopteran pests, either alone or in combination with selected members of the *Alphabaculovirus* genus. *Epinotia aporema* granulovirus (EpapGV) is a fast killing betabaculovirus that infects the bean shoot borer (*E. aporema*) and is a promising biopesticide. Because occlusion bodies (OBs) play a key role in baculovirus horizontal transmission, we investigated the composition of EpapGV OBs. Using mass spectrometry-based proteomics we could identify 56 proteins that are included in the OBs during the final stages of larval infection. Our data provides experimental validation of several annotated hypothetical coding sequences. Proteogenomic mapping against genomic sequence detected a previously unannotated ac*110*-like core gene and a putative translation fusion product of ORFs *epap48* and *epap49*. Comparative studies of the proteomes available for the family *Baculoviridae* highlight the conservation of core gene products as parts of the occluded virion. Two proteins specific for betabaculoviruses (Epap48 and Epap95) are incorporated into OBs. Moreover, quantification based on emPAI values showed that Epap95 is one of the most abundant components of EpapGV OBs.

Introduction

The family *Baculoviridae* comprises a diverse group of large double stranded DNA

28 viruses that infect larvae of the insect orders *Lepidoptera*, *Hymenoptera* and *Diptera*
29 [1]. Baculovirus have a rod shaped, enveloped virion with a circular genome ranging
30 from 80 to 180 kbp [2]. Virions are found in the environment embedded in a
31 proteinaceous matrix that forms occlusion bodies (OBs), a phenotype that is resistant
32 to desiccation and UV radiation. OBs on leaves that are consumed by foraging larvae
33 reach the midgut and, after being dissolved at high pH, release the occlusion derived
34 viruses (ODVs), which initiate infection of the epithelial cells. These infected cells
35 produce budded viruses (BVs) that disseminate the infection systemically [3]. Based on
36 OBs morphology, baculoviruses were first classified in two groups:
37 Nucleopolyhedrovirus (NPV) and Granulovirus (GV) [1]. Later, they were taxonomically
38 divided into four genera: *Alphabaculovirus* (lepidopteran-specific NPV),
39 *Betabaculovirus* (lepidopteran-specific GV), *Gammabaculovirus* (hymenopteran-
40 specific NPV) and *Deltabaculovirus* (dipteran-specific NPV) [1].
41 Among different entomopathogenic viruses, the baculoviruses have received most of
42 the attention due to their narrow host range which makes them safe pesticides. The
43 majority of commercial products are based on virus isolates that belong to the genera
44 *Alphabaculovirus* and *Betabaculovirus* [4]. The bean shoot borer (*Epinotia aporema*) is
45 an oligophagous pest that attacks soybean crops [5]. A poliorganotropic fast killing
46 betabaculovirus for this species, *Epinotia aporema* granulovirus (EpapGV), has been
47 discovered and sequenced by our group [6, 7]. In order to improve our understanding
48 of the infectious process we set out to analyze the protein content of EpapGV OB using
49 a proteomic approach.
50 Mass spectrometry-based (MS) proteomics represents a powerful technique to
51 interrogate the structural landscape of viral particles [8]. In addition to direct protein
52 identification, spectral data derived from proteomic experiments can be used to
53 identify novel features within genomic and transcriptomic datasets. This

54 proteogenomic methodology is independent of reference annotation, thus providing
55 excellent means for the refinement of gene models and the discovery of novel protein
56 coding sequences [9].
57 Virion proteomics has been applied to study several DNA virus families (*Ascoviridae*
58 [10], *Herpesviridae* [11], *Iridoviridae* [12], *Nudiviridae* [13] and *Poxviridae* [14]). In
59 relation with the present study, eight ODV proteomes of baculoviruses have been
60 analyzed (AcMNPV [15], AgMNPV [16], ChchNPV [17], HearNPV [18], MabrNPV [19],
61 ClanGV [20], PiraGV [21] and CuniNPV [22]). These datasets point at a complex virion
62 comprising a large number of proteins involved in virion morphogenesis, OBs
63 formation and infection of insect midgut epithelial cells.
64 In this work we examined the protein content of EpapGV OBs using MS-based shotgun
65 proteomics in order to describe the composition of this virion phenotype. A total of 56
66 viral proteins from EpapGV OBs were identified, the majority of which are conserved
67 components among the members of the family *Baculoviridae* and few are
68 betabaculovirus-specific proteins. Comparative proteomics of baculovirus showed a
69 set of core gene products present in the majority of proteomes analyzed.

70 Materials and Methods

71 *Larvae and virus*

72 Larvae of the bean shoot borer (*Epinotia aporema*), were collected from field in the
73 experimental station of the Instituto Nacional de Tecnología Agropecuaria (INTA) and
74 reared in our laboratory with an artificial diet and controlled light cycle (16 hours of
75 light). The strain used in this study was EpapGV (Refseq ID NC_018875), collected in
76 Oliveros (Santa Fe, Argentina) [6].
77

78 *Occlusion bodies (OBs) production and purification*

79 Fourth instar *E. aporema* larvae were infected *per os* using artificial diet contaminated
80 with a solution containing EpapGV OBs. Dying larvae with signs of infection were
81 stored and processed as described previously [7]. Briefly, infected larvae were stored
82 in distilled water and later homogenized in a Dounce homogenizer. The resulting
83 solution was filtered through three layers of cheesecloth to eliminate insoluble insect
84 debris. This extract was clarified by three steps of centrifugation at 10000 x g for 10
85 minutes followed by a wash with 0.05% v/v SDS solution. Clarified solution was
86 subjected to ultracentrifugation in a continuous 30-60% w/w sucrose gradient (50000 x
87 g, one hour, 4°C, Beckman SW 41 Ti rotor). The whitish/opalescent band corresponding
88 to OBs was collected, diluted 10-fold in distilled water and pelleted by centrifugation at
89 14000 x g for 10 minutes. The final pellet was resuspended in distilled water and
90 stored frozen at -20°C. Two biological independent samples were processed. Total
91 protein mass in the sample was quantified using the Bradford assay [23].
92
93 *Mass spectrometry analysis*
94 Protein digestion and analysis were performed at the Proteomics Core Facility
95 CEQUIBIEM, at the University of Buenos Aires/CONICET (National Research Council) as
96 follows: protein samples were reduced with 10 mM dithiothreitol in 50 mM
97 ammonium bicarbonate pH 8 (45 min, 56°C) and carbamidomethylated with 20 mM
98 iodoacetamide in the same solvent (40 min, room temperature, in darkness). This
99 protein solution was precipitated with 0.2 volumes of 100% w/v trichloroacetic acid
100 (Sigma) at -20 °C for at least two hours and centrifuged at 12000 x g for 10 min (4°C).
101 The pellet was washed twice with ice-cold acetone and dried at room temperature.
102 Proteins were resuspended in 50 mM ammonium bicarbonate pH 8 and digested with
103 trypsin (Promega V5111). The resulting peptides were desalted with ZipTip C18
104 columns (Millipore).

105 The digests were analyzed by nanoLC-MS/MS in a Thermo Scientific Q Exactive Mass
106 Spectrometer coupled to a nanoHPLC EASY-nLC 1000 (Thermo Scientific). For the LC-
107 MS/MS analysis, approximately 1 µg of peptides was loaded onto the column and
108 eluted for 120 minutes using a reverse phase column (C18, 2 µm x 10 nm particle size,
109 50 µm x 150 mm) Easy-Spray Column PepMap RSLC (P/N ES801) suitable for separating
110 complex mixtures of peptides with a high degree of resolution. The flow rate used for
111 the nano-column was 300 nL min^{-1} and the solvent range from 7% B (5 min) to 35% B
112 (120 min). Solvent A was 0.1% formic acid in water whereas B was 0.1% formic acid in
113 acetonitrile. The injection volume was 2 µL. The MS equipment has a high collision
114 dissociation cell (HCD) for fragmentation and an Orbitrap analyzer (Thermo Scientific,
115 Q-Exactive). A voltage of 3.5 kV was used for Electro Spray Ionization (Thermo
116 Scientific, EASY-SPRAY).
117 XCalibur 3.0.63 (Thermo Scientific) software was used for data acquisition and
118 equipment configuration that allows peptide identification at the same time of their
119 chromatographic separation. Full-scan mass spectra were acquired in the Orbitrap
120 analyzer. The scanned mass range was 400-1800 m/z, at a resolution of 70000 at 400
121 m/z and the 12 most intense ions in each cycle, were sequentially isolated, fragmented
122 by HCD and measured in the Orbitrap analyzer. Peptides with a charge of +1 or with
123 unassigned charge state were excluded from fragmentation for MS2.
124
125 *Analysis of MS data*
126 Q Exactive raw data was processed using Proteome Discoverer™ software (version
127 2.1.1.21, Thermo Scientific) and searched against EpapGV protein database
128 downloaded from NCBI (accession number NC_018875, National Center for
129 Biotechnology Information; www.ncbi.nlm.nih.gov) digested with trypsin with a
130 maximum of one missed cleavage per peptide. Proteome Discoverer™ searches were

131 performed with a precursor mass tolerance of 10 ppm and product ion tolerance of
132 0.05 Da. Static modifications were set to carbamidomethylation of Cys, and dynamic
133 modifications were set to oxidation of Met and N-terminal acetylation. Protein hits
134 were filtered for high confidence peptide matches with a maximum protein and
135 peptide false discovery rate of 1% calculated using a reverse database strategy. The
136 exponentially modified protein abundance index (emPAI) was calculated automatically
137 by Proteome Discoverer™ software and used to estimate the relative abundance of
138 identified proteins within the sample.
139
140 *Non annotated peptides search*
141 The complete genome sequence of EpapGV was translated *in silico* in all six frames
142 using the Mascot search software. Spectral data was searched and all peptides hits
143 were filtered to discard matches in previously annotated ORFs. The remaining peptides
144 were mapped to the corresponding genomic position. Search for putative unannotated
145 ORFs was done extending peptide hits until a stop codon was found at C-terminus, and
146 a start or stop codon for the N-terminus. Homologous sequences were searched using
147 the TBLASTN tool against all baculovirus genomes.
148
149 *Orthologs clustering*
150 A database comprising all the ODV proteins detected in baculoviruses was generated
151 using previous proteomic data sets [15-22]. The software BLASTP [24] and HHMER [25]
152 were used to identify groups of orthologous proteins (orthogroups) among different
153 proteomes by reciprocal best hits.
154 **Results**
155 *Structural components of the EpapGV OB*

156 We determined the composition of purified EpapGV OBs employing a shotgun
157 proteomic approach. The peptide mixture was separated by liquid chromatography
158 and analyzed with tandem mass spectrometry (LC-MS/MS). This approach was used to
159 avoid protein loss associated with SDS-PAGE gel extraction. We detected 56 proteins in
160 our purified EpapGV OBs samples. Genes encoding these proteins comprise 43.93% of
161 EpapGV total number of annotated ORFs (Fig 1), showing that a large part of the viral
162 genome codes for structural proteins. A total of 10 proteins (Epap10, Epap62, Epap71,
163 Epap123, LEF6, P6.9, Hel-1, P18, DNA Polymerase and DNA Ligase) were detected with
164 only a single peptide, which might be related to low molar proportions of these
165 polypeptides in the sample (Table 1). As additional evidence for the identification of
166 these proteins, we checked the presence of several ion products belonging to the
167 theoretical *b* and *y* spectral ions series for these peptides. The full list of proteins is
168 shown in Table 1. In our samples we were unable to detect PIF3 and desmoplakin, two
169 core gene products which have been confirmed in other virions by MS and western
170 blot [15]. This could be attributed to proteolytic degradation, low protein level or
171 deficient ionization of these proteins in our samples.
172
173
174 **Fig 1. Genomic localization of ORFs coding for proteins found in EpapGV OBs**
175 Proteins identified from spectral data (green arrows) were mapped to their respective
176 genomic coordinate (grey line). The novel identified Ac110-like peptide is highlighted
177 in red script. The baculovirus collinearity region is shown in black.
178
179
180 **Table 1. Proteins detected in EpapGV OBs**

ORF	Protein	NCBI Protein Id.	Size (aa)	% Coverage	# Peptides	emPAI	% emPAI
1	Granulin	YP_006908509.1	248	60,48	25	1995261	857918

5	P78/83	YP_006908513.1	137	16,06	2	0,33	0,14
6	PK1	YP_006908514.1	276	30,43	9	3,44	1,48
10	Epap10	YP_006908518.1	90	23,33	1	0,33	0,14
14	EFP	YP_006908522.1	541	5,18	1	0,08	0,03
21	PEP2	YP_006908529.1	142	45,07	5	4,62	1,99
22	PEP/P10	YP_006908530.1	308	48,70	8	9	3,87
25	PEP1	YP_006908533.1	178	37,64	6	5,31	2,28
27	**PIF5**	YP_006908535.1	354	31,07	7	5,58	2,40
28	**Ac142**	YP_006908536.1	457	44,86	18	4,84	2,08
29	**ODV-E18**	YP_006908537.1	88	45,45	6	176,83	76,03
31	v-Cath	YP_006908539.1	329	5,77	2	0,29	0,12
39	ODV-E66	YP_006908547.1	654	33,64	14	5,31	2,28
40	Epap40	YP_006908548.1	102	75,49	6	16,78	7,22
47	**PIF2**	YP_006908555.1	374	20,05	7	0,69	0,30
48	Epap48	YP_006908556.1	446	37,67	13	2,54	1,09
49	Epap49	YP_006908557.1	1465	29,83	35	2,88	1,24
52	v-Ubi	YP_006908560.1	93	33,33	3	1,37	0,59
53	**ODV-EC43**	YP_006908561.1	348	47,41	12	6,20	2,67
58	SOD	YP_006908566.1	183	55,19	9	24,12	10,37
59	**PIF0**	YP_006908567.1	653	11,02	5	0,47	0,20
62	Epap62	YP_006908570.1	106	10,38	1	0,39	0,17
66	P24	YP_006908574.1	165	27,88	3	0,87	0,37
69	**PIF1**	YP_006908577.1	538	7,99	3	0,52	0,22
71	Epap71	YP_006908579.1	104	6,73	1	0,47	0,20
74	LEF6	YP_006908582.1	82	12,19	1	0,47	0,20
78	**P48/45**	YP_006908586.1	380	6,58	2	0,10	0,04
79	P12	YP_006908587.1	115	38,26	3	4,62	1,99
80	**P40**	YP_006908588.1	373	25,20	9	1,68	0,72
81	**P6.9**	YP_006908589.1	56	14,29	1	2,16	0,93
83	**38K**	YP_006908591.1	295	26,44	5	1,45	0,62
84	**PIF4**	YP_006908592.1	162	20,99	3	0,67	0,29
85	**Hel-1**	YP_006908593.1	1085	1,29	1	0	0,00
86	**ODV-E25**	YP_006908594.1	213	43,19	7	9	3,87
87	**P18**	YP_006908595.1	158	5,06	1	0	0.00
88	**P33**	YP_006908596.1	254	36,61	7	1,98	0,85
90	ChaB	YP_006908598.1	75	45,33	2	2,98	1,28
92	**VP39**	YP_006908600.1	293	75,43	21	232,27	100,00
93	**ODV-EC27**	YP_006908601.1	284	24,65	8	3,39	1,46
94	BRO	YP_006908602.1	359	5,85	2	0,23	0,10
95	Epap95	YP_006908603.1	73	69,86	5	176,83	76,03
96	**PIF8**	YP_006908604.1	567	14,10	7	1,22	0,52
98	**Ac81**	YP_006908606.1	191	23,04	5	1,61	0,69
99	**GP41**	YP_006908607.1	286	74,82	23	87,59	37,66
100	**Ac78**	YP_006908608.1	88	44,32	2	16,78	7,22
101	**VLF-1**	YP_006908609.1	368	35,87	11	3,06	1,32
103	Ac75	YP_006908611.1	149	56,38	9	7,11	3,06
106	**DNA Pol**	YP_006908614.1	1068	2,72	1	0	0.00
109	**PIF6**	YP_006908617.1	148	41,22	5	2,59	1,11
113	FP25K	YP_006908621.1	146	19,86	3	0,23	0,10
115	DNA Lig	YP_006908623.1	534	4,87	1	0,08	0,03
123	Epap123	YP_006908630.1	102	6,87	1	0,47	0,20

126	Epap126	YP_006908633.1	347	45,82	11	3,49	1,50
127	Epap127	YP_006908634.1	69	30,43	2	1,15	0,49
129	**VP1054**	YP_006908636.1	344	11,05	2	0,1	0,04
133	ME53	YP_006908640.1	373	9,91	2	0,22	0,09
-	**Ac110**	This study	47	29.79	1	-	-

% Coverage: percentage of the protein sequence covered by identified peptides.

emPAI: exponentially modified Protein Abundance Index.

ORF: Open Reading Frame, as numbered in EpapGV genome map published by Ferrelli *et al* [7].

Peptides: number of individual peptides identified for each protein

Core gene products are in bold characters.

In addition to identifying the components of the OBs, we estimated the relative abundance of each protein; to this end we calculated the emPAI value proposed by Ishihama *et al* [26] for each protein. The emPAI value for the major capsid protein VP39 was used to normalize protein abundance (Table 1). Taking a cutoff value of at least 10 % VP39 emPAI, the most abundant proteins are GP41, Granulin, ODV-E18, SOD and Epap95, together with VP39. The major capsid component VP39, the tegument protein GP41 and the major component of OB matrix granulin were expected to be among the most abundant proteins due to their known structural function. ODV-E18 ortholog in AcMNPV is an essential protein for BV production that also localizes to the ODV membrane [27]. Cu-Zn superoxide dismutase (SOD) activity in virion preparations of Chlorovirus PBCV-1 has been recently associated with reactive oxygen species reduction during the early stages of virus infection [28]. Finally, Epap95 a protein with orthologs in all the members of the genus *Betabaculovirus*, has been consistently detected in the granuloviruses of *Clostera anachoreta* (ClanGV) and *Pieris rapae* (PiraGV) as a component within ODVs.

Betabaculovirus gene content remains poorly characterized, with a large number of hypothetical genes predicted by phylogenomics methods. Some of these genes lack

205 *bona fide* experimental evidence to confirm the actual existence of their putative
206 protein products. Our proteomic data confirmed the presence of translation products
207 for 10 hypothetical proteins annotated in the genome of EpapGV, namely, Epap10,
208 Epap40, Epap48, Epap49, Epap62, Epap71, Epap95, Epap123, Epap126 and Epap127.
209
210 *Short peptides encoded in EpapGV genome that do not belong to annotated ORFs*
211 To identify possible unannotated proteins, we searched our spectral data against a
212 theoretical database comprising all translation products predicted in the six reading
213 frames of EpapGV genome sequence (we included all possible ORFs, without
214 introducing a minimal size criterion). We detected seven peptides that mapped to the
215 EpapGV genome but did not belong to the set of annotated ORFs [7]. Their sequence
216 and genomic location are detailed in S1 Appendix. One of these peptides matches an
217 unannotated 47 amino acids long ORF overlapping *epap51* but in the opposite
218 orientation. We further examined the presence of this novel ORF in other members of
219 the family *Baculoviridae* and found that it is an ortholog of the core gene *ac110* [29].
220 This gene has been described as the *per os* infectivity factor 7 (*pif7*) and its product has
221 only been detected in the proteome of HearNPV ODV [18] and EpapGV (this study).
222 Genomic localization and orientation of this *ac110*-like gene is conserved within
223 *Betabaculovirus*, providing additional evidence about its evolutionary conservation.
224 The remaining six peptides overlap with annotated ORFs (*chitinase*, *dna ligase* and
225 *granulin*) or intergenic regions. Two peptides were found between ORFs *epap48* and
226 *epap49* and one peptide between *epap61* and *epap62*. TBLASTN was used to find
227 putative homologous unannotated peptides in other baculovirus genomes. Only the
228 peptides overlapping with *chitinase* and *granulin* are conserved in homologous *loci* in
229 GV and NPV genomes (S1 Appendix).
230 Remarkably, peptides between *epap48* and *epap49* almost cover the entire 145 bp

231 intergenic sequence (Fig 2). *Epap48* encodes a 446 amino acid long protein that is
232 conserved in the betabaculoviruses. The putative translation product of *epap49* is a
233 large protein composed of 1465 residues with no orthologs detected in other
234 baculoviruses. Mapped peptides are located in the same reading frame as the
235 translation product of *epap49*, but no methionine codon has been found in frame (Fig
236 2). One hypothesis that could explain the presence of these peptides is that Epap48
237 and Epap49 may be expressed as a fusion protein due to a putative +1 frameshifting
238 event near the C-terminus of Epap48; further experimental validation of this potential
239 fusion protein will be needed to confirm this hypothesis.
240
241
242 **Fig 2. Putative fusion protein Epap48-Epap49**
243 (A) Genomic locus containing *epap48* (green) and *epap49* (blue) genes. The two
244 peptides detected by MS inside the intergenic region are depicted in purple. (B)
245 Genome sequence and translation frame for each gene. Start and stop codons are
246 shown in red (nucleotide numbers are those from NCBI accession number
247 NC_018875).
248
249
250 *Conservation of structural proteins in the family Baculoviridae*
251 The reports of ODV proteomes belonging to several baculoviruses were used to
252 evaluate the conservation of the viral particle composition in this family. To date, eight
253 proteomic studies were carried out on ODV, including five members of the genus
254 *Alphabaculovirus* (AcMNPV, AgMNPV, ChchNPV, MabrNPV and HearNPV), two of the
255 genus *Betabaculovirus* (ClanGV and PiraGV) and one of *Deltabaculovirus* (CuniNPV).
256 Our study expands this data with the proteins present in the EpapGV OBs. Sequences

257 of proteins detected in occluded virions of baculovirus were used to construct groups
258 of orthologous proteins (S1 Table). For each of these orthogroups we scored the
259 number of proteomes in which they are present as a measure of their conservation.
260 We assigned them a class based in the phylogenetic conservation of their coding
261 sequence (core, lepidopteran-specific, genus-specific and virus specific) (Fig 3A). Most
262 conserved protein groups (present in a larger number of proteomes) are enriched in
263 core and lepidopteran-specific gene products. In contrast, proteins specific to a small
264 set of proteomes are encoded by genus-specific and virus-specific genes.
265 The betabaculovirus proteomes (EpapGV, ClanGV and PiraGV) were compared using a
266 Venn diagram (Fig 3B). From the proteins present in all three viruses, BRO, Epap48,
267 Epap95 and Epap126 are the only orthogroups without functional characterization.
268 Interestingly, Epap95 is one of the most abundant proteins according to emPAI values.
269 Additionally, Epap126 is shared between group II alphabaculoviruses and
270 betabaculoviruses (except for ClanGV) (S1 Table). On the other hand, Epap10, Epap49
271 and Epap62 are proteins unique to EpapGV OBs. Remarkably, *epap10* orthologs are
272 encoded only in five alphabaculoviruses that infect insects of the family *Tortricidae*,
273 *Choristoneura fumiferana* NPV, *Choristoneura occidentalis* NPV, *Choristoneura*
274 *rosaceana* NPV, *Cryptophlebia peltastica* NPV and *Epiphyas postvittana* NPV. This could
275 be the product of an ancestral horizontal gene transfer between alphabaculoviruses
276 and betabaculoviruses that coinfected the same host, based on gene conservation
277 evidence.
278
279
280 **Fig 3. Baculovirus proteome comparison.** (A) Protein conservation in baculovirus
281 occluded virion proteomes. Protein orthogroups derived from proteomics datasets
282 were scored according to the number of proteomes in which they were detected.

283 Gene class distribution (core genes, lepidopteran baculovirus-specific, genus-specific,
284 specie-specific) of orthologs groups within *Baculoviridae* is highlighted in different
285 colours. (B) Proteins detected in proteomes of betabaculoviruses were grouped in sets
286 of orthologs and represented using a Venn diagram. A set of 34 proteins is present in
287 all three viruses [20, 21, this study]; core gene products are highlighted in bold. Two of
288 these protein clusters being specific of *Betabaculovirus* (Epap48 and Epap95).

289

290

291 **Discussion**

292 Occluded virions are responsible for baculovirus primary infection. Proteome of OBs is
293 related with oral infectivity, providing relevant information about conserved
294 components potentially associated with midgut infection. Until now, the proteomes of
295 ClanGV and PiraGV ODVs have been interrogated using MS-based techniques [20, 21].
296 These viral species are phylogenetically distant to EpapGV [7]. We explored possible
297 divergence in protein composition employing a bottom-up proteomic approach to
298 characterize the protein content of EpapGV OBs. A diagram of the EpapGV virion
299 particle summarizing qualitative and semi-quantitative composition is shown in Fig 4.
300 Virion components can be grouped in five classes based in their localization: 18
301 nucleocapsid proteins, 15 ODV envelope proteins, 5 occlusion matrix proteins, 1
302 tegument protein and 17 proteins of undefined localization. Comparisons across virion
303 proteomes available for members of the family *Baculoviridae* highlighted the
304 conservation of several structural components forming the mature virion. On the other
305 hand, comparative genomics highlight the conservation of a collinear genomic region
306 for lepidopteran-infecting baculoviruses [30]. Combined genomics and proteomics
307 information suggests that this *locus*, compared to the rest of genome, is densely

308 populated by protein coding sequences corresponding predominantly to structural
309 polypeptides (Fig 1 and S1 Fig). Intriguingly, the product of the core gene desmoplakin
310 could not be detected in the betabaculovirus structural proteomes but it has been
311 reported for alphabaculoviruses; we do not know if this is related to a different
312 localization of this protein within betabaculovirus or due to technical reasons. In
313 AcMNPV, desmoplakin has been implied in the segregation of nucleocapsids destined
314 to build BV (which are ubiquitinated) and ODV (non ubiquitinated) [31].

315

316

317 **Fig 4. Schematic model of EpapGV OB.** Qualitative and semi-quantitative virion model
318 based on our proteomic data and localization described in published reports. Protein
319 levels were estimated using the emPAI value and expressed as relative value with
320 respect to the major capsid protein VP39.

321

322

323 It has been previously reported that proteins related to viral DNA metabolism and DNA
324 binding capacity may be retained in the virion [15]. In the present study we could
325 identify the DNA polymerase, DNA ligase and Helicase-1 in OBs. For other
326 baculoviruses IE1, Alk-Exo, LEF1 and LEF3 have been detected also. This reinforces the
327 idea that the viral DNA is associated with various proteins (in addition to the major
328 condensing protein P6.9) inside the viral capsid.

329 The envelope that surrounds the ODV morphotype is especially adapted for primary
330 infection of the insect midgut and presents a complex complement of proteins. These
331 can be classified in two functional groups, those required for virion envelopment and

332 those related with oral infectivity. Envelope morphogenesis begins with the formation
333 of intranuclear microvesicles (IMV) derived from the inner nuclear membrane and the
334 association with viral capsids. The ODV membrane proteins Ac75 and P18 are
335 necessary for the generation of these IMV [32, 33]. Subsequently, envelopment of
336 assembled nucleocapsids requires the ODV proteins Ac78, Ac81, Ac142, ODV-E25,
337 ODV-EC43, P33 and P48 to form mature OBs [34-40] . On the other hand, several ODV
338 membrane proteins are members of the PIF complex (PIF0, PIF1, PIF2, PIF3, PIF4, PIF5,
339 PIF6 and PIF8); this molecular complex is the main effector of oral infection in the
340 insect midgut. These proteins are encoded by core genes conserved in all the members
341 of the *Baculoviridae* family [41].

342 The biological relevance of the betabaculovirus-specific orthogroups Epap48 and
343 Epap95 within OBs is currently unknown. Moreover, the high content of Epap95 in the
344 OBs may also be biologically relevant. On the other hand, Epap126 orthogroup is
345 present in group II alphabaculoviruses and betabaculoviruses, which represents a
346 conserved protein potentially involved in oral infection.

347 Baculovirus genomes are densely populated with coding sequences (overlapping in
348 several cases) and contain short intergenic regions [2]. A recent study has described
349 the transcriptional landscape of baculovirus infection, demonstrating the existence of
350 several polycistronic and overlapping viral transcripts [42]. Together with other
351 technologies, proteogenomic mapping is a valuable tool to improve the annotation of
352 these complex coding regions. This approach has been used in proteome research for
353 several virus families [43], but was applied only for one baculovirus, AgMNPV [44]. We
354 identified seven peptides that do not map to previously annotated coding regions. One
355 of these peptides turned to be an ortholog of *ac110*; this ORFs overlapped with the
356 coding sequence of *epap51*. Moreover, the presence of peptides derived from
357 alternative frames inside the coding regions of *granulin* and *chitinase* raises the

358 question about the underlying complexity of baculovirus transcription and translation
359 processes.

360 Surprisingly, two unmapped peptides were found to be encoded in the intergenic
361 region of *epap48* and *epap49* and suggest the presence of a putative fusion product
362 between these proteins. Epap49 is the largest protein annotated in EpapGV genome; it
363 is 1465 amino acids long. As previously reported, it was difficult to annotate this as a
364 hypothetical protein due to its atypically large size, absence of homologous proteins in
365 Genbank and lack of known promoter motifs [7]. Also, it was noted that large proteins
366 were coded in similar locations in the genomes of ChocGV and HearGV, 1144 and
367 1279 amino acids long, respectively [45, 46]. In the case of ChocGV it was not
368 annotated in the genome [45] and in HearGV it was found to be a fusion of ORFs
369 homologous to XecnGV 47 and 48 [46]. In this study, we found evidence that Epap49 is
370 actually translated.

371 **Conclusion**

372 The protein composition of EpapGV OBs was interrogated using an MS-based
373 proteomic approach. A total of 56 proteins have been detected in the EpapGV
374 occluded virion, suggesting the presence of a highly conserved protein profile in
375 baculoviral OBs. We identified Epap95, a betabaculovirs-specific protein, as a highly
376 abundant capsid component. This protein represents an interesting candidate for
377 further functional studies to explore its role in betabaculovirus pathogenesis. Through
378 proteogenomic search we could detect a non-annotated coding region with a high
379 degree of sequence identity to *ac110*. In addition, our data strongly suggest the
380 translation of a putative fusion protein involving Epap48 and Epap49. Our study
381 highlight the usefulness of MS proteomics to characterize the protein complement of

the viral particle and the possibility to improve genome annotation through experimental evidence for translation of predicted coding regions.

Acknowledgements

The authors thank Dr. Silvia Margarita Moreno and Dr. María Pía Valacco, from the Centro de Estudios Químicos y Biológicos por Espectrometría de Masas (CEQUIBIEM-CONICET-FCEN-UBA), for their help with sample preparation protocols, data acquisition and subsequent analysis. This work was supported by grants from the Agencia Nacional de Promoción Científica y Tecnológica (ANPCyT) and UNLP to Víctor Romanowski.

391 **References**

392 1. Harrison RL, Herniou EA, Jehle JA, Theilmann DA, Burand JP, Becnel JJ, et al. ICTV
393 Virus Taxonomy Profile: Baculoviridae. Journal of General Virology.
394 2018;99(9):1185-1186. pmid: 29947603.
395 2. van Oers MM, Vlak JM. Baculovirus genomics. Curr Drug Targets. 2007;8(10),
396 1051–68. pmid: 17979665
397 3. Passarelli AL. Barriers to success: how baculoviruses establish efficient systemic
398 infections. Virology. 2011;411(2):383-92. pmid: 21300392
399 4. Haase S, Sciocco-Cap A, Romanowski V. Baculovirus insecticides in Latin America:
400 historical overview, current status and future perspectives. Viruses. 2015;7:2230–
401 67. pmid: 25941826
402 5. Sánchez NE, Pereyra PC. Neotropical soybean budborer, Crocidosema aporema
403 (Walsingham, 1914) (Lepidoptera: Tortricidae). In J. L. Capinera (Ed.), Encyclopedia
404 of Entomology. Dordrecht: Springer Netherlands. 2008. pp. 2587–2588. doi:
405 https://doi.org/10.1007/978-1-4020-6359-6_2186
406 6. Sciocco-Cap A, Parola AD, Goldberg AV, Ghiringhelli PD, Romanowski V.
407 Characterization of a granulovirus isolated from Epinotia aporema Wals.
408 (Lepidoptera: Tortricidae) larvae. Appl Environ Microbiol. 2001;67(8):3702-6.
409 pmid: 11472950
410 7. Ferrelli ML, Salvador R, Biedma M, Berretta M, Haase S, Sciocco-Cap, A, et al.
411 Genome of Epinotia aporema granulovirus (EpapGV), a polyorganotropic fast
412 killing betabaculovirus with a novel thymidylate kinase gene. BMC Genomics.
413 2012;13(1):548. pmid: 23051685
414 8. Greco TM, Diner BA, Cristea IM. The impact of mass spectrometry–based
415 proteomics on fundamental discoveries in virology. Annu Rev Virol. 2014;1(1):581-
416 604. pmid: 26958735
417 9. Nesvizhskii AI. Proteogenomics: concepts, applications and computational
418 strategies. Nat Methods. 2014;11(11):1114–1125. pmid: 25357241
419 10. Tan Y, Bideshi DK, Johnson JJ, Bigot Y, Federici BA. Proteomic analysis of the
420 Spodoptera frugiperda ascovirus 1a virion reveals 21 proteins. J Gen Virol.
421 2009;90:359–365. pmid: 19141444
422 11. Vidick S, Leroy B, Palmeira L, Machiels B, Mast J, François S,et al. Proteomic
423 characterization of murid herpesvirus 4 extracellular virions. PLoS ONE.
424 2013;8(12):e83842. pmid: 24386290
425 12. Ince IA, Boeren SA, Van Oers MM, Vervoort JJM, Vlak JM. Proteomic analysis of
426 Chilo iridescent virus. Virology. 2010;405(1):253–258. pmid: 20598335
427 13. Bézier A, Harichaux G, Musset K, Labas V, Herniou EA. Qualitative proteomic
428 analysis of Tipula oleracea nudivirus occlusion bodies. J Gen Virol. 2017;98(2):284–
429 295. pmid: 28284235
430 14. Doellinger J, Schaade L, Nitsche A. Comparison of the Cowpox Virus and Vaccinia
431 Virus mature virion proteome: analysis of the species- and strain-specific
432 proteome. PLOS ONE. 2015;10(11):e0141527. pmid: 26556597
433 15. Braunagel SC, Russell WK, Rosas-Acosta G, Russell DH, Summers MD.
434 Determination of the protein composition of the occlusion-derived virus of
435 Autographa californica nucleopolyhedrovirus. Proc Natl Acad Sci USA.
436 2003;100(17):9797-802. pmid: 12904572
437 16. Braconi CT, Ardisson-Araújo DM, Paes Leme AF, Oliveira JV, Pauletti BA, Garcia-
438 Maruniak A, et al. Proteomic analyses of baculovirus Anticarsia gemmatalis
439 multiple nucleopolyhedrovirus budded and occluded virus. J Gen Virol.
440 2014;95:980–989. pmid: 24443474
441 17. Xu F, Ince IA, Boeren S, Vlak JM, Van Oers MM. Protein composition of the

occlusion derived virus of Chrysodeixis chalcites nucleopolyhedrovirus. Virus Res. 2011;158(1-2):1–7. pmid: 21354223

18. Hou D, Zhang L, Deng F, Fang W, Wang R, Liu X, et al. Comparative proteomics reveal fundamental structural and functional differences between the two progeny phenotypes of a baculovirus. J Virol. 2013;87(2):829–39. pmid: 23115289
19. Hou D, Chen X, Zhang LK. Proteomic analysis of Mamestra Brassicae Nucleopolyhedrovirus progeny virions from two different hosts. PLOS ONE. 2016; 11(4):e0153365. pmid: 27058368
20. Zhang, X., Yin, X., Liang, Z., & Shao, X. Proteomic analysis of the occlusion-derived virus of Clostera anachoreta granulovirus. J Gen Virol. 2015;96(8):2394–2404. pmid: 25872743
21. Wang XF, Zhang BQ, Xu HJ, Cui YJ, Xu YP, Zhang MJ, et al. ODV-associated proteins of the Pieris rapae granulovirus. J Proteome Res. 2011;10(6):2817–2827. pmid: 21517121
22. Perera O, Green TB, Stevens SM Jr, White S, Becnel JJ. Proteins associated with Culex nigripalpus nucleopolyhedrovirus occluded virions. J Virol. 2007;81(9):4585-90. pmid: 17301145
23. Bradford MM. A rapid and sensitive method for the quantitation of microgram quantities of protein utilizing the principle of protein-dye binding. Anal. Biochem. 1976;72(1–2):248–54. pmid: 942051
24. Altschul SF, Gish W, Miller W, Myers EW, Lipman DJ. Basic local alignment search tool. J. Mol. Biol. 1990;215(3):403-410. pmid: 2231712
25. Eddy SR. Accelerated Profile HMM Searches. PLoS Comput Biol. 2011;7(10):e1002195. pmid: 22039361
26. Ishihama Y, Oda Y, Tabata T, Sato T, Nagasu T, Rappsilber J, et al. Exponentially modified protein abundance index (emPAI) for estimation of absolute protein amount in proteomics by the number of sequenced peptides per protein. Mol Cell Proteomics. 2005;4(9):1265–1272. pmid: 15958392
27. McCarthy CB, Theilmann DA. AcMNPV ac143 (odv-e18) is essential for mediating budded virus production and is the 30th baculovirus core gene. Virology. 2008;375(1):277-291. pmid: 18328526
28. Kang M, Duncan GA, Kuszynski C, Oyler G, Zheng J, Becker DF, et al. Chlorovirus PBCV-1 encodes an active copper-zinc superoxide dismutase. J Virol. 2014;88(21):12541-12550. pmid: 25142578
29. Javed MA, Biswas S, Willis LG, Harris S, Pritchard C, van Oers MM, et al. Autographa californica multiple nucleopolyhedrovirus AC83 is a per os infectivity factor (PIF) protein required for occlusion-derived virus (ODV) and budded virus nucleocapsid assembly as well as assembly of the PIF complex in ODV envelopes. J Virol. 2017;91(5):e02115-16. pmid: 28031365
30. Zhu Z, Yin F, Liu X, Hou D, Wang J, Zhang L, et al. Genome sequence and analysis of Buzura suppressaria nucleopolyhedrovirus: a group II Alphabaculovirus. PloS One. 2014;9(1):e86450. pmid: 24475121
31. Biswas S, Willis LG, Fang M, Nie Y, Theilmann DA. Autographa californica nucleopolyhedrovirus AC141 (Exon0), a potential E3 ubiquitin ligase, interacts with viral ubiquitin and AC66 to facilitate nucleocapsid egress. J Virol. 2018;92(3):e01713-17 pmid: 29142135
32. Shi A, Hu Z, Zuo Y, Wang Y, Wu W, Yuan M, et al. Autographa californica nucleopolyhedrovirus ac75 is required for the nuclear egress of nucleocapsids and intranuclear microvesicle formation. Journal of Virology. 2017;92(4):e01509-17. pmid: 29212928
33. Yuan M, Huang Z, Wei D, Hu Z, Yang K, Pang Y. Identification of Autographa californica nucleopolyhedrovirus ac93 as a core gene and its requirement for

494 intranuclear microvesicle formation and nuclear egress of nucleocapsids. J Virol.
495 2011;85(22):11664–74. pmid: 21880748
496 34. Tao XY, Choi JY, Kim WJ, Lee JH, Liu Q, Kim SE, et al. The Autographa californica
497 multiple nucleopolyhedrovirus ORF78 is essential for budded virus production and
498 general occlusion body formation. J Virol. 2013;87(15):8441–8450. pmid:
499 23698311
500 35. Dong F, Wang J, Deng R, Wang X. Autographa californica multiple
501 nucleopolyhedrovirus gene ac81 is required for nucleocapsid envelopment. Virus
502 Res. 2016;221:47–57. pmid: 27212683
503 36. McCarthy CB, Dai X, Donly C, Theilmann DA. Autographa californica multiple
504 nucleopolyhedrovirus ac142, a core gene that is essential for BV production and
505 ODV envelopment. Virology. 2008;372(2):325–339. pmid: 18045640
506 37. Chen L, Hu X, Xiang X, Yu S, Yang R, Wu X. Autographa californica multiple
507 nucleopolyhedrovirus odv-e25 (Ac94) is required for budded virus infectivity and
508 occlusion-derived virus formation. Arch Virol. 2012;157(4):617–625. pmid:
509 22218963
510 38. Alfonso V, Maroniche GA, Reca SR, López MG, del Vas M, Taboga O. AcMNPV Core
511 gene ac109 is required for budded virion transport to the nucleus and for
512 occlusion of viral Prpgeny. PLoS ONE. 2012;7(9):e46146. pmid: 23049963
513 39. Wu W, Passarelli AL. Autographa californica multiple nucleopolyhedrovirus Ac92
514 (ORF92, P33) is required for budded virus production and multiply enveloped
515 occlusion-derived virus formation. J Virol. 2010;84(23):12351–61. pmid: 20861245
516 40. Yuan M, Wu W, Liu C, Wang Y, Hu Z, Yang K, et al. A highly conserved baculovirus
517 gene p48 (ac103) is essential for BV production and ODV envelopment. Virology.
518 2008;379(1):87–96. pmid: 18656219
519 41. Boogaard B, van Oers MM, van Lent JWM. An advanced view on baculovirus per
520 os infectivity factors. Insects. 2018;9(3):E84 pmid: 30018247
521 42. Moldován N, Tombácz D, Szűcs A, Csabai Z, Balázs Z, Kis E, et al. Third-generation
522 sequencing reveals extensive polycistronism and transcriptional overlapping in a
523 baculovirus. Sci. Rep. 2018;8(1):8604. pmid: 29872099
524 43. Leroy B, Gillet L, Vanderplasschen A, Wattiez R. Structural proteomics of
525 herpesviruses. Viruses. 2016;8(2):50. pmid: 26907323
526 44. Brito AF, Braconi CT, Weidmann M, Dilcher M, Alves JMP, Gruber A, et al. The
527 Pangenome of the Anticarsia gemmatalis Multiple Nucleopolyhedrovirus
528 (AgMNPV). Genome Biol Evol. 2015;8(1):94–108. pmid: 26615220
529 45. Escasa SR, Lauzon HAM, Mathur AC, Krell PJ, Arif BM. Sequence analysis of the
530 Choristoneura occidentalis granulovirus genome. J Gen Virol. 2006;87(7):1917–33.
531 pmid:16760394.
532 46. Harrison RL, Popham HJR. Genomic sequence analysis of a granulovirus isolated
533 from the Old World bollworm, Helicoverpa armigera. Virus Genes.
534 2008;36(3):565–81. pmid:18418706.

535

536 ## Supplementary information

537 **S1 Appendix.** EpapGV unannotated peptides detected by MS.

538 **S1 Figure.** Parity plot of sequences coding for structural proteins present in AcMNPV,

539 ChchNPV and PiraGV against EpapGV.

540 **S1 Table.** Proteomic profiles of baculovirus occluded virions proteomes.

541

542

543

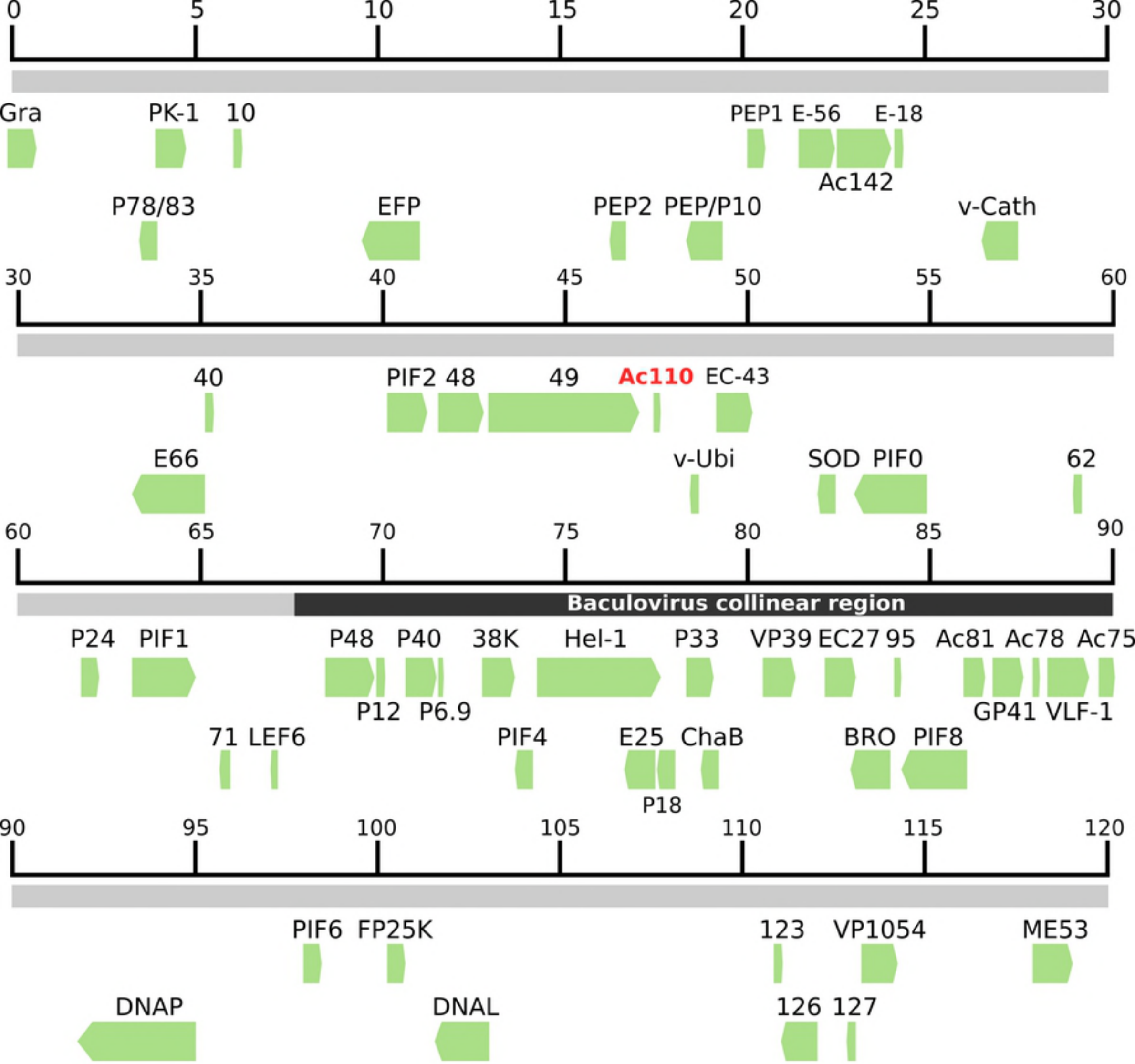
0
5
10
15
20
25
30
Gra
PK-1
10
PEP1
E-56
E-18
Ac142
P78/83
EFP
PEP2
PEP/P10
v-Cath
30
35
40
45
50
55
60
40
PIF2
48
49
Ac110
EC-43
E66
v-Ubi
SOD
PIF0
62
60
65
70
75
80
85
90
Baculovirus collinear region
P24
PIF1
P48
P40
38K
Hel-1
P33
VP39
EC27
95
Ac81
Ac78
Ac75
P12
P6.9
GP41
VLF-1
71
LEF6
PIF4
E25
ChaB
BRO
PIF8
P18
90
95
100
105
110
115
120
PIF6
FP25K
123
VP1054
ME53
DNAP
DNAL
126
127

Figure

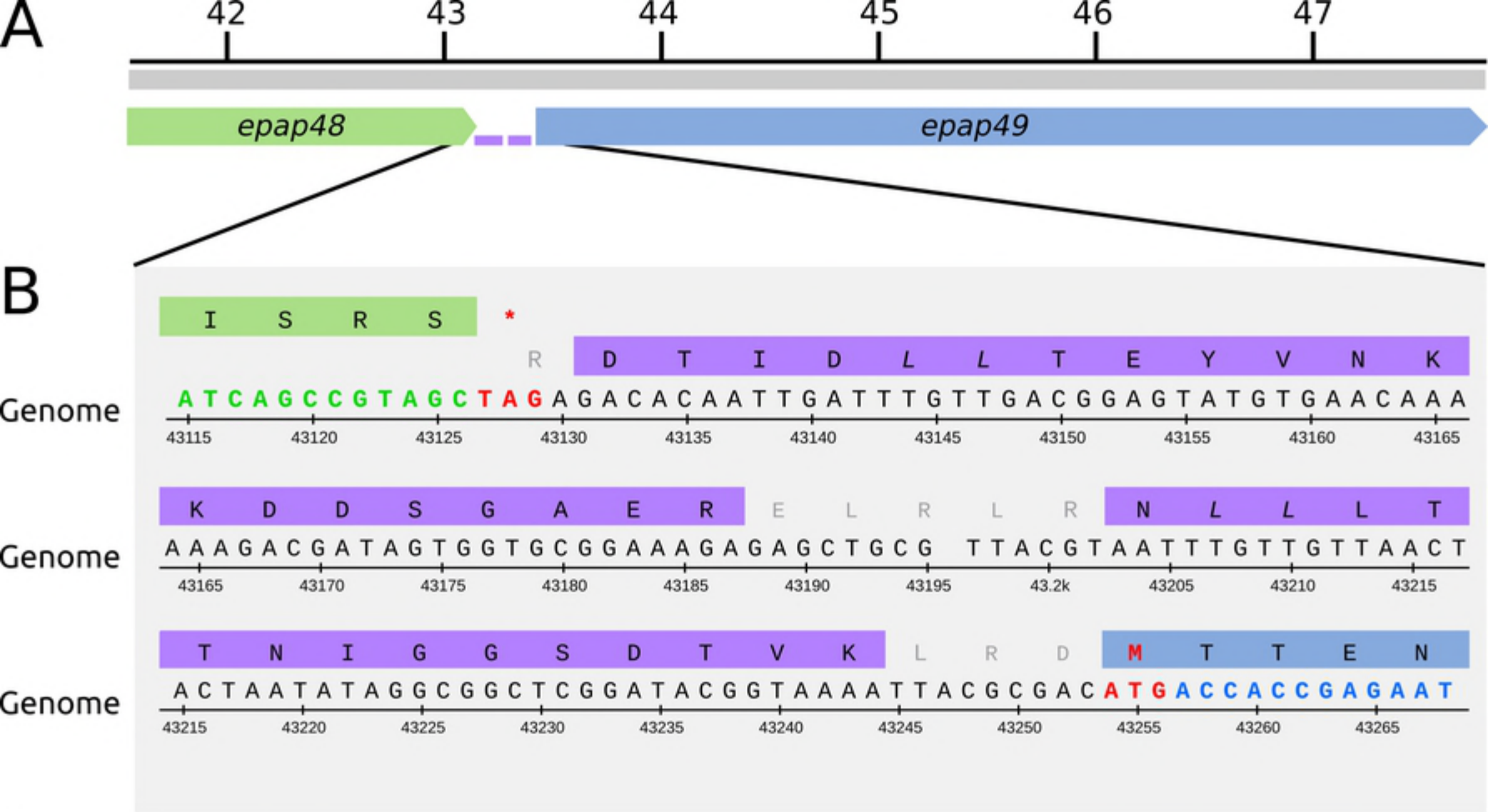
A
42
43
44
45
46
47
epap48
epap49
B
I S R S *
R D T I D L L T E Y V N K
Genome
ATCAGCCGTAGCTAGAGACACAATTGATTTGTTGACGGAGTATGTGAACAAA
43115 43120 43125 43130 43135 43140 43145 43150 43155 43160 43165
K D D S G A E R E L R L R N L L L T
Genome
AAAGACGATAGTGGTGCGGAAAGAGAGCTGCG TTACGTAATTTGTTGTTAACT
43165 43170 43175 43180 43185 43190 43195 43.2k 43205 43210 43215
T N I G G S D T V K L R D M T T E N
Genome
ACTAATATAGGCGGCTCGGATACGGTAAAATTACGCGACATGACCACCGAGAAT
43215 43220 43225 43230 43235 43240 43245 43250 43255 43260 43265

Figure

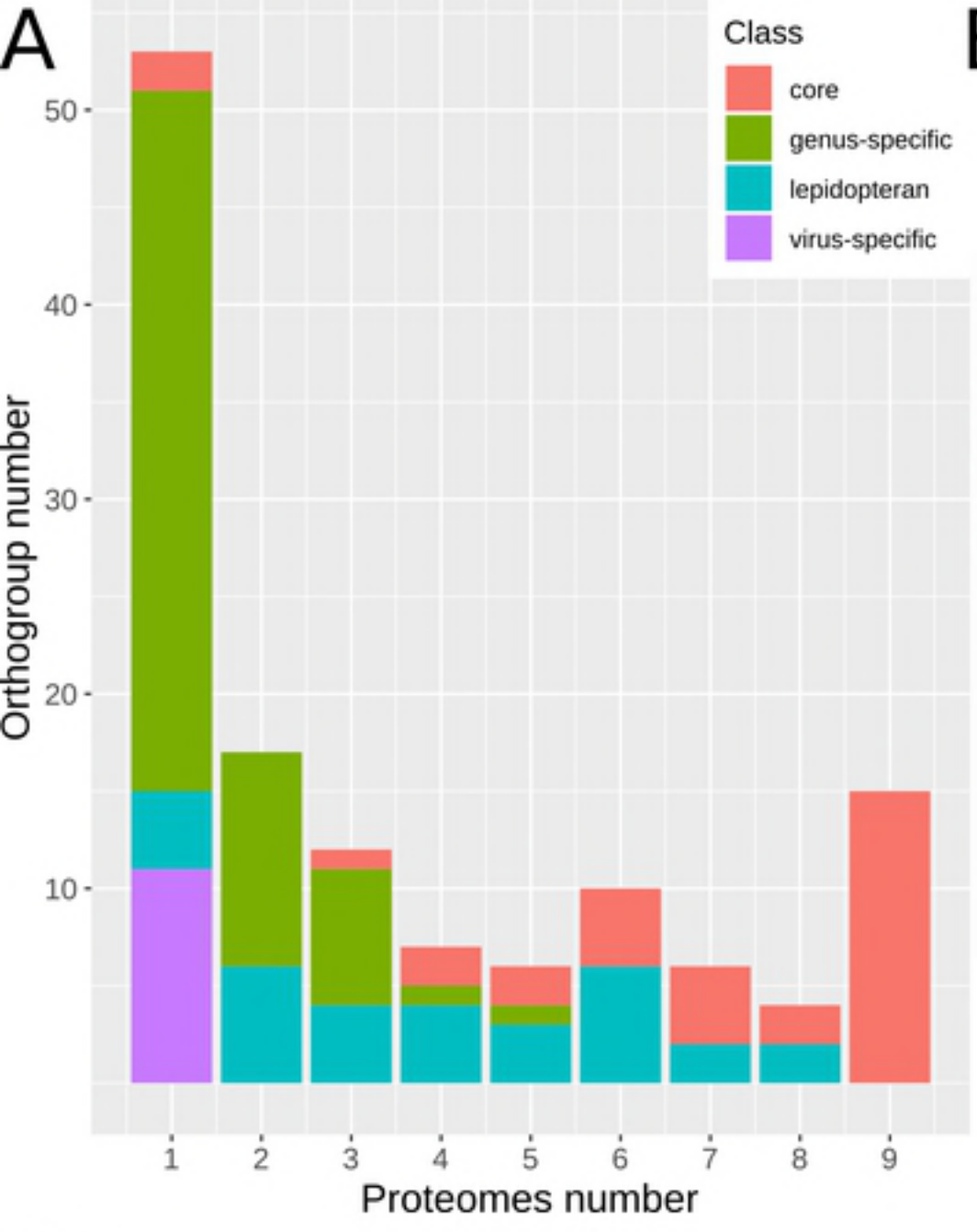
A
Class
core
genus-specific
lepidopteran
virus-specific
Orthogroup number
50
40
30
20
10
1
2
3
4
5
6
7
8
9
Proteomes number

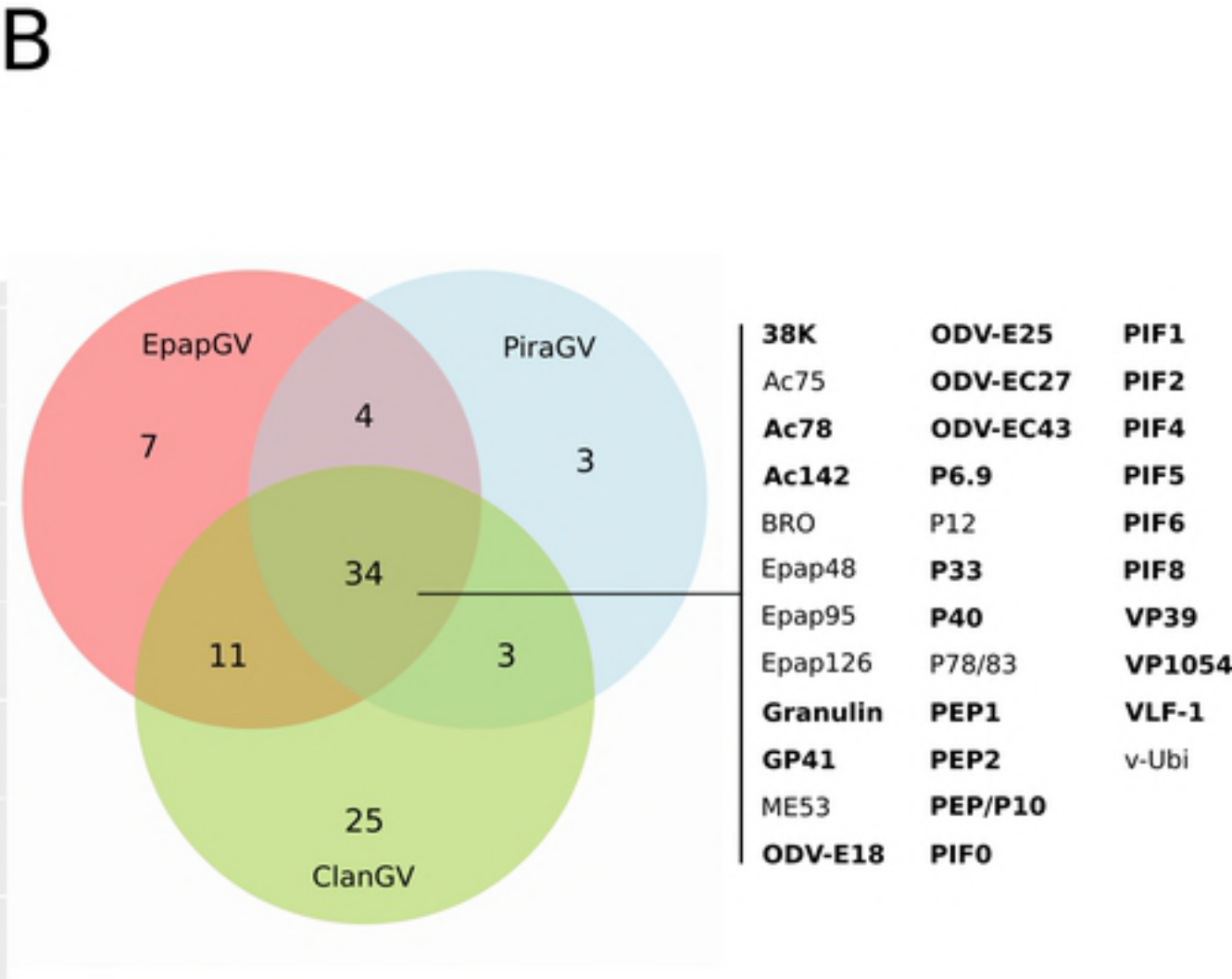
B
EpapGV
PiraGV
ClanGV
7
4
3
34
11
3
25
38K
Ac75
Ac78
Ac142
BRO
Epap48
Epap95
Epap126
Granulin
GP41
ME53
ODV-E18
ODV-E25
ODV-EC27
ODV-EC43
P6.9
P12
P33
P40
P78/83
PEP1
PEP2
PEP/P10
PIF0
PIF1
PIF2
PIF4
PIF5
PIF6
PIF8
VP39
VP1054
VLF-1
v-Ubi

Figure

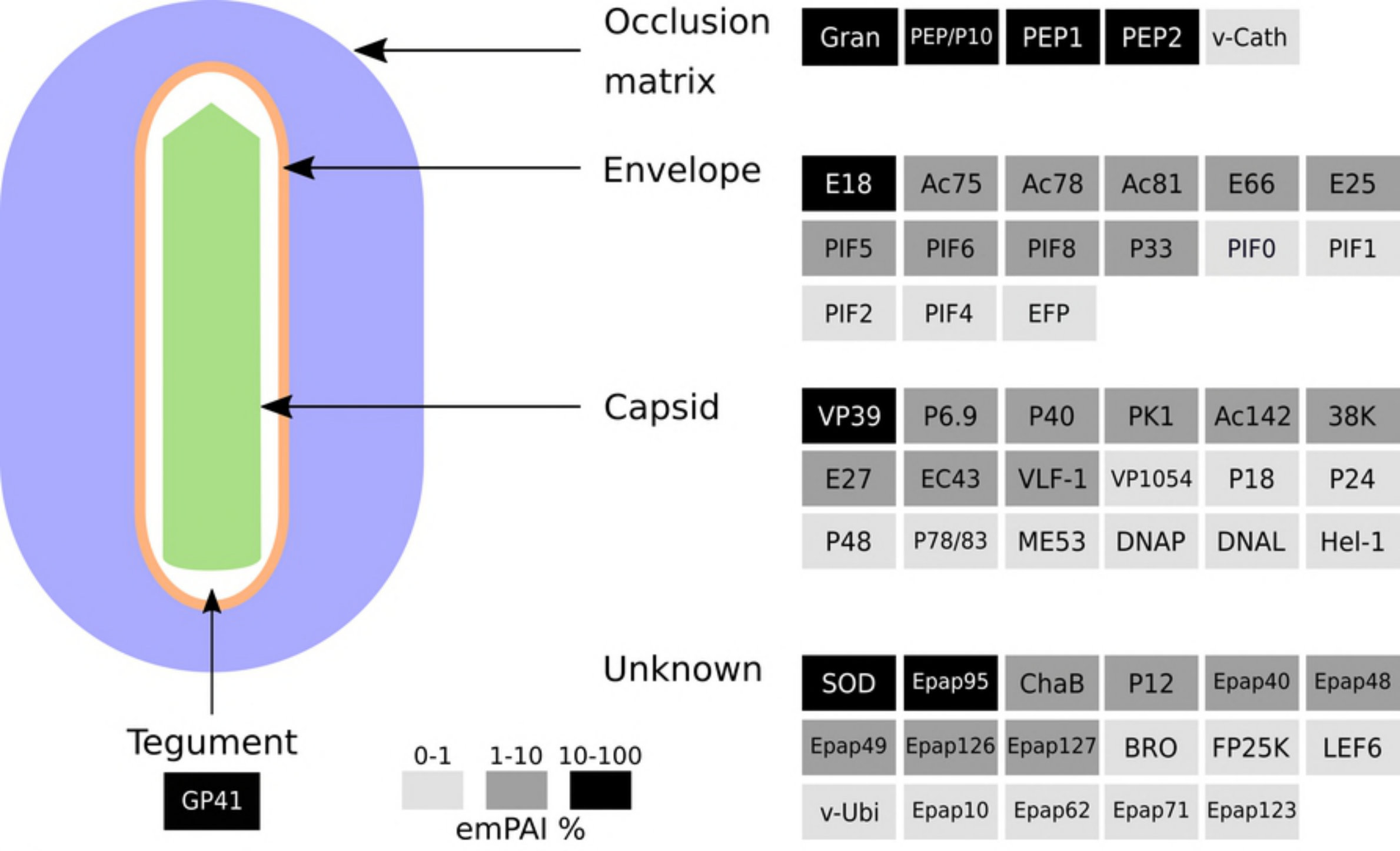
Occlusion matrix
Gran
PEP/P10
PEP1
PEP2
v-Cath
Envelope
E18
Ac75
Ac78
Ac81
E66
E25
PIF5
PIF6
PIF8
P33
PIF0
PIF1
PIF2
PIF4
EFP
Capsid
VP39
P6.9
P40
PK1
Ac142
38K
E27
EC43
VLF-1
VP1054
P18
P24
P48
P78/83
ME53
DNAP
DNAL
Hel-1
Unknown
SOD
Epap95
ChaB
P12
Epap40
Epap48
Epap49
Epap126
Epap127
BRO
FP25K
LEF6
v-Ubi
Epap10
Epap62
Epap71
Epap123
Tegument
GP41
0-1
1-10
10-100
emPAI %

Figure